

Superconductivity and anomalous transport in SrPd_2Ge_2 single crystals

N. H. Sung,¹ Jong-Soo Rhyee,³ and B. K. Cho^{1,2}

¹*School of Materials Science and Engineering, Gwangju Institute of Science and Technology (GIST), Gwangju 500-712, Korea*

²*Department of Nanobio Materials and Electronics, Gwangju Institute of Science and Technology (GIST), Gwangju 500-712, Korea*

³*Department of Applied Physics, Kyung Hee University, Yong-In 446-701, Korea*

(Received 12 September 2010; published 10 March 2011)

Superconducting ternary germanide SrPd_2Ge_2 single crystals ($T_c = 2.70$ K) with a ThCr_2Si_2 -type structure were synthesized using a high-temperature metal flux method. Superconductivity was confirmed by temperature- and magnetic-field-dependent magnetization, electrical resistivity, and heat capacity measurements. Here, weak anisotropy in superconductivity was observed both parallel and perpendicular to the crystallographic c axis. Various superconductivity parameters, such as lower and upper critical fields, the temperature gradient of the upper critical field, and coherence length were estimated, and the upper critical value at $T = 0$ K was found to be much larger than the value for the polycrystalline sample. In addition, the anomalous temperature dependence of resistivity was observed in a temperature range of $T_c (=2.70 \text{ K}) \leq T \leq T^* (=2.90 \text{ K})$ when a current was applied along the c axis, whereas the only slope change occurred at T^* with a current perpendicular to the c axis, prior to a sharp superconducting transition at T_c .

DOI: 10.1103/PhysRevB.83.094511

PACS number(s): 74.25.Ha, 74.25.fc, 74.25.Bt

I. INTRODUCTION

Tetragonal ThCr_2Si_2 -type structure compounds have been extensively researched over the past few decades owing to the noteworthy properties of rare-earth intermetallic compounds, such as their superconductivity, heavy fermionic and non-Fermi liquid behavior, and quantum criticality.¹⁻³ In particular, superconductivity in pnictide compounds, $AE\text{TM}_2\text{Pn}_2$ (AE = alkaline earth, TM = transition metal, and Pn = pnictogen), has been increasingly studied, with a relatively high superconducting transition temperature ($T_c \sim 38$ K) achieved when the compound was doped with holes.^{4,5} After this discovery, the ThCr_2Si_2 -type structure has received considerable attention in the solid-state physics and chemistry communities, and the structure has been considered an important clue for discovering noble high T_c superconductors. As such, significant effort has been expended in attempts to identify correlations between atomic structures, electronic and magnetic properties, and superconductivity; all devoted to further understanding the origin of superconductivity. Most pnictide compounds, which show superconductivity, contain either Fe or Ni. Because of its strong magnetic moment, Fe (or Ni) generally has been considered an exotic material, resulting in complicated interactions with superconductivity, either being detrimental to or enhancing superconductivity. Therefore, for the study of superconductivity in terms of pure atomic and electronic variations, there has been an attempt to obtain noble pnictide superconductors without magnetic elements.^{6,7}

Recently, type-II superconductivity in polycrystalline samples of SrPd_2Ge_2 ($T_c = 3.04$ K) was reported,⁸ which has a ThCr_2Si_2 -type structure without any magnetic elements or pnictogen. Therefore, despite the lower T_c in this compound, as compared to that in ThCr_2Si_2 -type iron-pnictide compounds, the SrPd_2Ge_2 compound would be a more suitable candidate for the investigation of the superconducting nature in ThCr_2Si_2 -type structures, as well as in the search for new superconducting compounds of the ThCr_2Si_2 -type structure. Thus, it would be of great interest to investigate physical properties of single-crystalline SrPd_2Ge_2 along specific crys-

tallographic directions. In this paper, large single crystals of SrPd_2Ge_2 were grown by the high-temperature metal flux method and were found to be superconducting from the magnetization, electrical resistivity, and heat capacity measurements. In addition, clear anisotropy in the temperature dependence of electronic transport near the superconducting transition temperature was also found.

II. EXPERIMENTAL DETAILS

Single SrPd_2Ge_2 crystals were grown by the high-temperature flux method, using PdGe as a self-flux. High-purity Sr (99.95%), Pd (99.99%), and Ge (99.999%) elements were used as the starting materials. Sr, Pd, and Ge pieces were placed in an alumina crucible together with an atomic ratio of $\text{Sr} : \text{Pd} : \text{Ge} = 1 : 5 : 5$. The entire process was performed in a glove box under an argon atmosphere. The assembly was then sealed in a quartz tube under $1/3$ atm Ar gas and placed vertically in a programmable box furnace. The furnace was heated to 1100°C at a rate of 200°C/h , kept for 2 days at 1100°C to ensure sufficient melting, and then cooled to 850°C at a rate of 3°C/h . Next, the tube was centrifuged to separate grown crystals from the flux, using quartz wool as a filter. As a result, we could get well-grown shiny platelike crystals of SrPd_2Ge_2 , which have a maximum dimension of $11 \times 7 \times 3 \text{ mm}^3$ [Fig. 1(a)]. The crystals could be easily cleaved with tweezers into small platelike pieces. The characterization of crystals was performed using a powder x-ray diffractometer (XRD; Rigaku, RINT2000), field-emission scanning electron microscopy (SEM; Hitachi S-4700), and energy-dispersive x-ray (EDX; Horiba 7200-H) spectroscopy. XRD was performed at room temperature and unit-cell parameters were refined using PowderCell software. Temperature- and field-dependent magnetizations of single crystals were measured by a superconducting quantum interference device magnetometer (SQUID; Quantum Design MPMS XL). Electrical resistivity was measured using a LR700 resistance bridge, combined with a SQUID temperature control system, and Epotek H20E silver epoxy was used to ensure the electrical contact of Pt wires

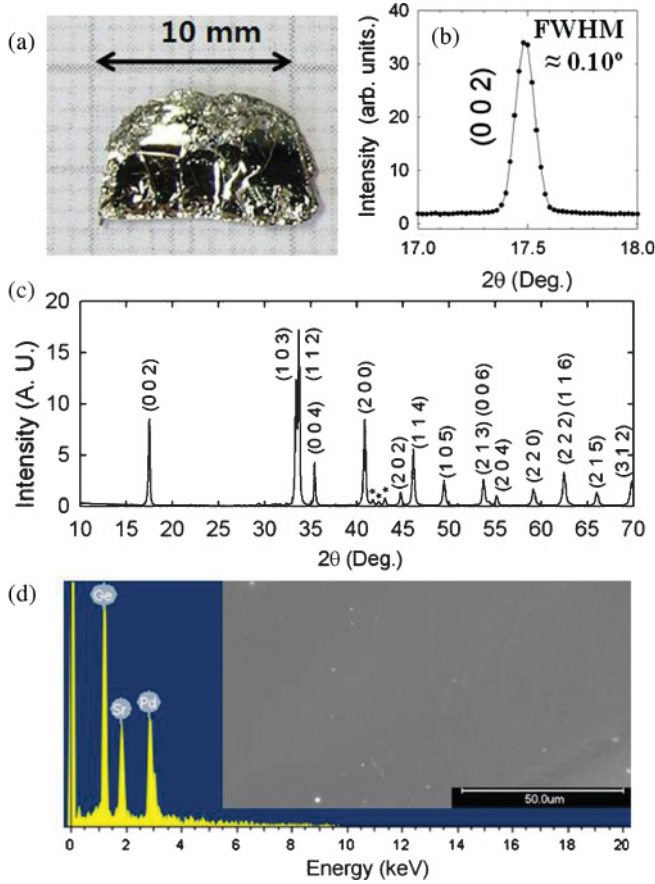


FIG. 1. (Color online) (a) Single crystal of SrPd_2Ge_2 , grown using the metal flux method. (b) Rocking curve of (0 0 2) reflection of the surface of platelike crystal SrPd_2Ge_2 , with dimensions of $\sim 2 \times 2 \times 0.05 \text{ mm}^3$. (c) Powder XRD pattern of pulverized single crystals and indexing. The peaks denoted by asterisks are from the self-flux PdGe as an impurity phase. (d) Characterization of a SrPd_2Ge_2 single crystal using scanning electron microscopy and energy-dispersive x ray.

on the sample surface. The superconducting volume fraction was estimated from zero-field cooling (ZFC) and field-cooling warmup (FCW) magnetization with $H = 2 \text{ Oe}$. Here, ZFC magnetization was measured with increasing temperatures in a field after cooling down to 2 K in the zero field, and FCW magnetization was measured with increasing the temperature in the same field. The electrical resistivity was measured using a four-probe method in a temperature range of 2–300 K. Heat capacity was measured using a Quantum Design physical property measurement system (PPMS) using the relaxation technique.

III. RESULTS AND DISCUSSION

The shiny flat surface of a cleaved single crystal was measured using XRD, with only (0 0 $2n$) ($n = \text{integer}$) reflections being detected from the 2θ scan, which indicates that the c axis is perpendicular to the cleaved surface. The full width at half maximum (FWHM) in the x-ray rocking curve of (0 0 2) was $\sim 0.10^\circ$, which shows the good crystallization of the samples [Fig. 1(b)]. Several crystals were collected and pulverized to measure powder XRD [Fig. 1(c)]. The major

peak pattern was identified as a ThCr_2Si_2 -type phase, and minor extra peaks from the PdGe phase were determined to originate from impurities possibly remaining on the crystal surfaces. The lattice parameters for the tetragonal system were determined to be $a = 4.4129(4) \text{ \AA}$ and $c = 10.1204(5) \text{ \AA}$, which are comparable to the parameters of the polycrystalline samples.⁸ Figure 1(d) shows the morphological and compositional characterizations of the surface of a SrPd_2Ge_2 single crystal. The SEM image shows a large and flat surface with minor impurities on it, and a quantitative analysis of the EDX spectra is used to estimate the composition of $\text{SrPd}_{1.99}\text{Ge}_{2.05}$, which is close to the ideal chemical composition of the crystal, within error range.

The temperature-dependent magnetization of a single crystal, with dimensions of $\sim 1.89 \times 2.97 \times 0.45 \text{ mm}^3$ and a mass of 9.6 mg, was measured and plotted in Fig. 2. Magnetization measurements, with the field parallel and perpendicular to the c axis in the ZFC and FCW processes, were performed with $H = 2 \text{ Oe}$. From the measurements, the superconducting transition temperature was found to be $T_c = 2.70 \text{ K}$ and bulk superconductivity was confirmed [Fig. 2(a)]. The transition width, ΔT_c , was found to be larger than that for polycrystalline

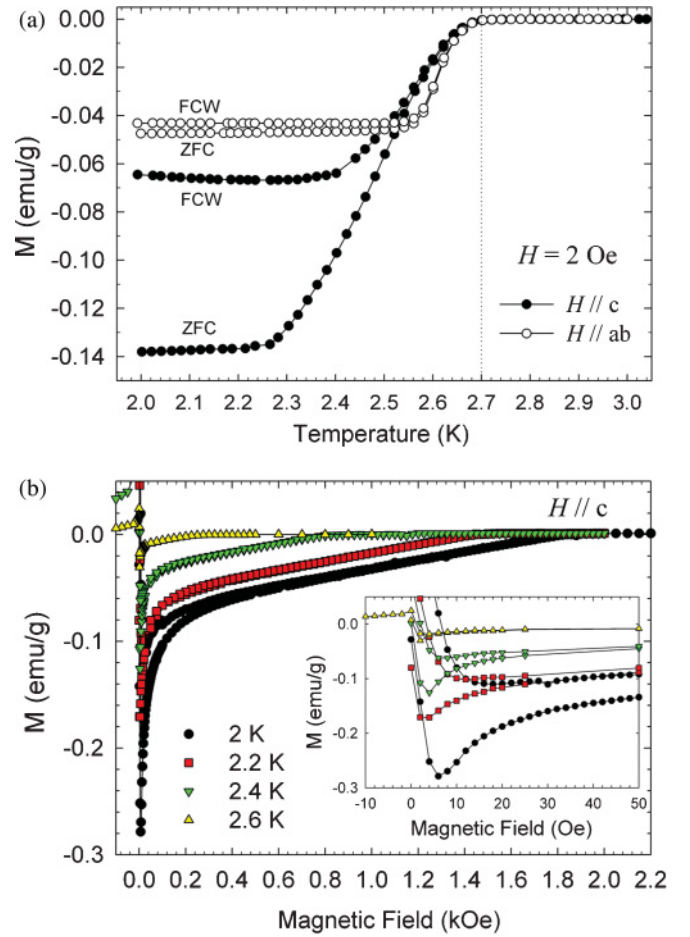


FIG. 2. (Color online) (a) Temperature dependence of magnetization of a SrPd_2Ge_2 single crystal with a field of 2 Oe, being parallel ($H \parallel c$) and perpendicular ($H \parallel ab$) to the c axis in both ZFC and FCW modes. (b) Isothermal magnetization of a SrPd_2Ge_2 single crystal at various temperatures with the field along the c axis. Inset: Expanded plot in a low-field region.

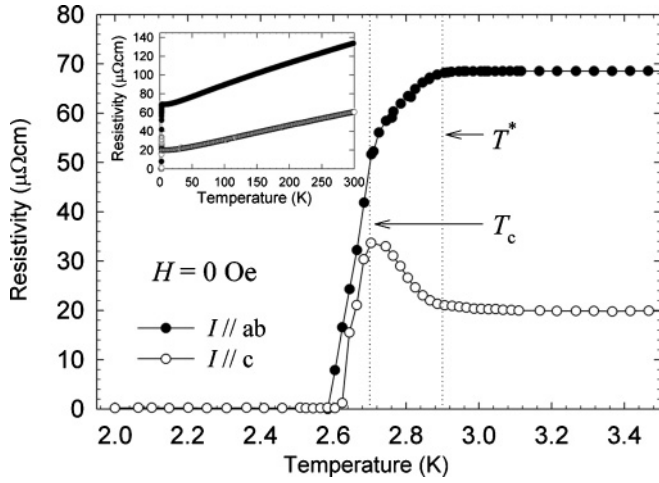


FIG. 3. Temperature dependence of electrical resistivity of SrPd_2Ge_2 single crystals with a current, parallel ($I \parallel c$) and perpendicular ($I \parallel ab$) to the c axis. Inset: Temperature-dependent resistivity up to $T = 300$ K.

samples.⁸ Such large ΔT_c can be caused by flux trapping and the superconducting glass state in SrPd_2Ge_2 such as cuprate superconductors.⁹ We observed the flux trapping after

the magnetic field was turned off at $T = 2$ K, as well as its nonexponential time decay. Moreover, an irreversible trajectory in the magnetization measurement was measured with changing temperature. Details of the flux trapping and superconducting glass state will be reported elsewhere. In addition, isothermal magnetization in terms of magnetic field was measured at various temperatures, as shown in Fig. 2(b). The M - H loop shows nearly ideal type-II superconducting behavior with a low H_{c1} value. The inset of Fig. 2(b) is an expanded plot in the low-field region, which shows the lower critical field H_{c1} to be less than 6 Oe at 2 K. In addition, small hysteresis, compared to the data of polycrystals,⁸ indicates the small value of critical current density and, equivalently, a weak vortex pinning, which is a typical characteristic of single-crystalline samples.

Figure 3 shows the temperature-dependent electrical resistivity in a zero field, with current directions being parallel and perpendicular to the c axis. As shown in the inset of Fig. 3, the resistivity in a normal state exhibits typical metallic behavior in a temperature range $3 \text{ K} \leq T \leq 300 \text{ K}$. For the measurement with the current parallel to the c axis, a schematic contact configuration was plotted in the inset of Fig. 4. Taking into account the geometrical contact configuration and small thickness of the crystal, the absolute value of resistivity

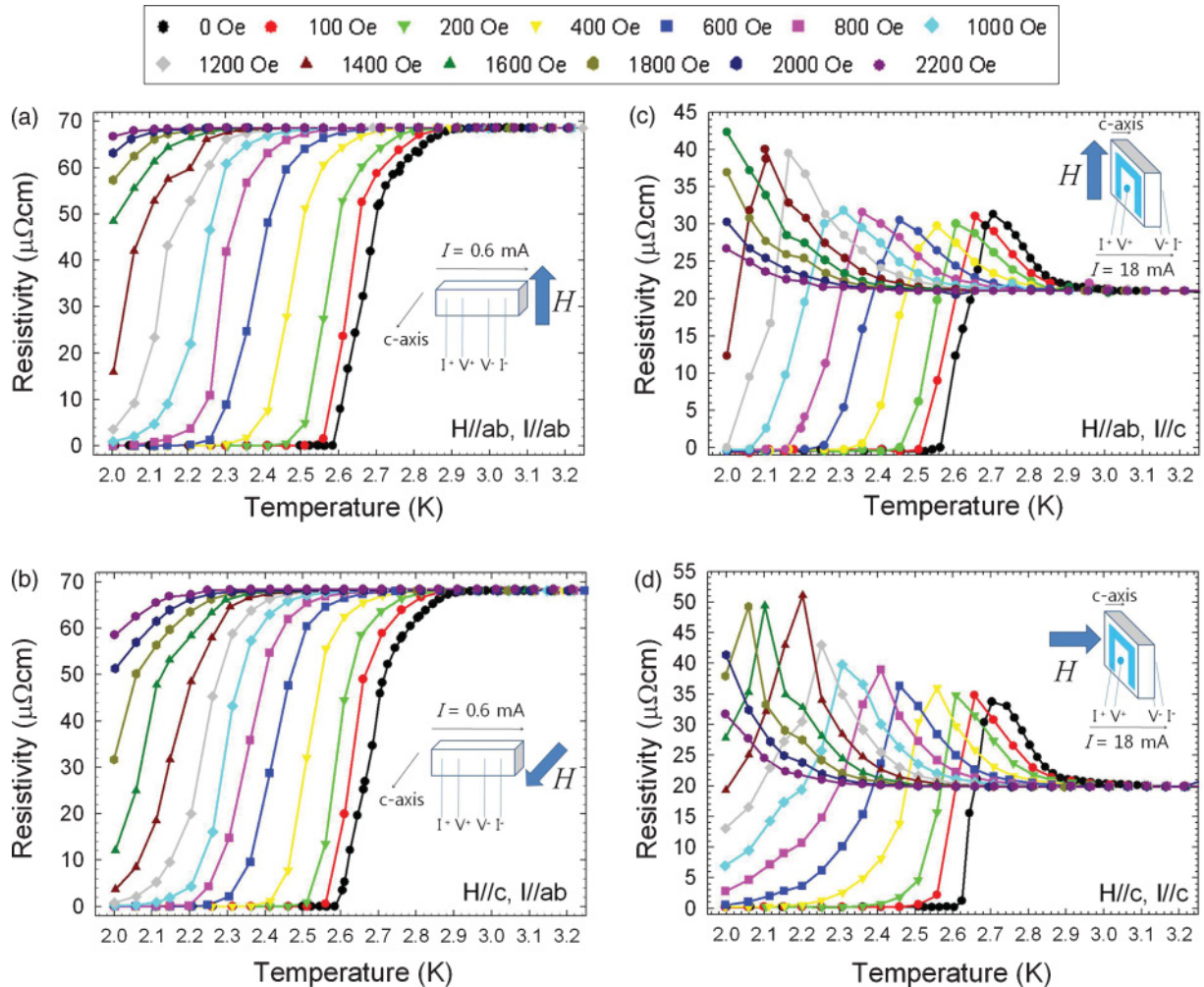


FIG. 4. (Color online) Temperature dependence of electrical resistivity of a SrPd_2Ge_2 single crystal at various magnetic field (H) and current (I) configurations, as indicated in the inset of each figure. Notation: Parallel ($\parallel c$) and perpendicular ($\parallel ab$) to the c axis.

along the c axis has significant error; as such, the difference between the absolute values of resistivity along and perpendicular to the c axis in the inset of Fig. 3 may have no physical meaning.

On the other hand, the temperature dependence of resistivity near the superconducting transition temperature shows a clear difference, as shown in Fig. 3. For the current perpendicular to the c axis, two sharp slope changes were found; one is the superconducting transition at $T_c = 2.70$ K, which corresponds to the transition temperature in the M - T curve [Fig. 2(a)], and the other is at $T^* = 2.90$ K. For the current parallel to the c axis, insulatorlike behavior of resistivity was found in the temperature range of $2.70 \text{ K} \leq T \leq 2.90 \text{ K}$, while a sharp superconducting transition also occurred at $T_c = 2.70$ K.

The temperature dependence of resistivity near the superconducting transition temperature, which was measured under various configurations of magnetic field and current direction, is plotted in Fig. 4. The current and magnetic-field directions are schematically plotted in the insets of Fig. 4, i.e., (a) $H \parallel ab$, $I \parallel ab$, (b) $H \parallel c$, $I \parallel ab$, (c) $H \parallel ab$, $I \parallel c$, and (d) $H \parallel c$, $I \parallel c$, and the contacts of current and voltage measurement were also plotted. For the current perpendicular to the c axis [Figs. 4(a) and 4(b)], the zero resistivity temperature was systematically suppressed with increasing magnetic field with negligible broadening of the superconducting transition width. For the current parallel to the c axis [Figs. 4(c) and 4(d)], both the superconducting transition and the peak position were systematically suppressed. From these results, it would appear that the height and width of the resistivity peak increase with increasing fields. Several crystals from the same batch were then selected to reproduce the resistivity measurements with a current parallel to the c axis and were found to show a similar behavior of resistivity, as shown in Figs. 4(c) and 4(d). Similar anomalous transport behavior, i.e., the anisotropic temperature dependence of resistivity between the intralayer and interlayer transport, was observed in other layered structure compounds, such as a high- T_c cuprate¹⁰ and $(\text{LaSe})_{1.14}(\text{NbSe}_2)$.¹¹ As described in Ref. 11, the peak effect in SrPd_2Ge_2 may be explained in terms of the correlation of the quasiparticle and Cooper-pair tunneling in the charge transport through the layers. Details on the origin of the resistivity peak in this study will be presented elsewhere.

It should be noted that the physical properties of single crystals were very sensitive to their growth conditions. For example, the single crystals, which were grown using In flux, showed neither superconductivity nor anisotropy in the temperature dependence near $T = 2.9$ K. It is not clear at present how the growth conditions, in particular, metal flux, caused such a dramatic change in the physical properties. Such flux dependency was also observed in SrFe_2As_2 single crystals, which showed superconductivity when prepared using self- (FeAs) flux,¹² but it had no superconductivity when it was prepared using metal (Sn) flux.¹³ This strongly suggests that the crystal growth using self-flux is essential for obtaining the intrinsic single crystals of pnictide compounds.

Figure 5 shows the specific heat, divided by temperature, C_p/T , for various magnetic fields, parallel to the c axis, in a temperature range of $2.0 \text{ K} \leq T \leq 3.5 \text{ K}$. The superconduct-

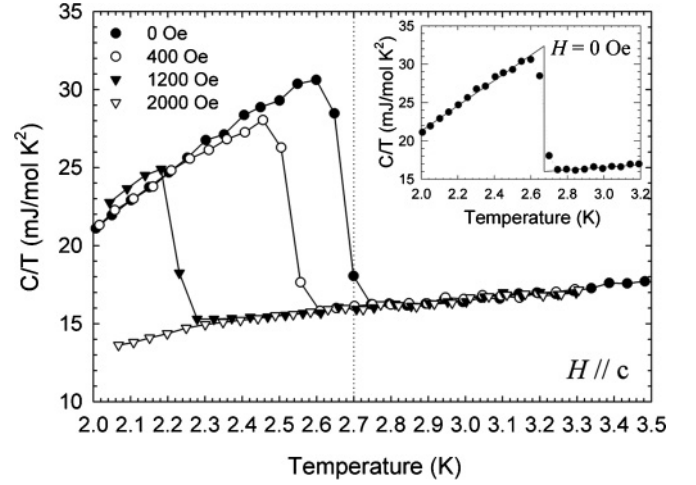


FIG. 5. Plot of specific heat C_p , divided by temperature T , in terms of T for a SrPd_2Ge_2 single crystal at various magnetic fields near the superconducting transition temperature. Inset: Line fitting to determine the superconducting transition temperature at the midpoint of jump.

ing transition temperature, $T_c = 2.70$ K, which was determined from M - T [Fig. 2(a)] and R - T (Fig. 3), corresponds to the onset of the specific heat jump, and the zero resistance temperature (Fig. 3) corresponds to the midpoint of the specific heat jump. As shown in the inset of Fig. 5, a superconducting transition temperature of $T_c^{\text{midpoint}} = 2.67$ K was extracted from an equal area construction, and the specific heat jump ΔC is equal to 43.8 mJ/K . With the field increase, the specific heat jump was systematically suppressed. Based on a fit of the data (not shown) from $T = 2.8$ to 8.9 K with $H = 0$ Oe to the equation $\frac{C}{T} = \gamma + \beta T^2 + \delta T^4$, the Sommerfeld coefficient $\gamma = 7.8 \text{ mJ/mol K}^2$ was obtained, which is comparable to the theoretical value $\gamma_{\text{cal}} = 6.84 \text{ mJ/mol K}^2$.¹⁴ Based on this value, the ratio of the specific heat jump at $T_c^{\text{midpoint}} = 2.67$ K to the electronic specific heat was estimated to be $\frac{\Delta C}{\gamma T_c} \cong 2.1$. This value is higher than the theoretical value of 1.43 for weak-coupling Bardeen-Cooper-Schrieffer (BCS) superconductivity, suggesting that the superconductivity of SrPd_2Ge_2 may be strongly coupled. In addition, the Debye temperature was also obtained to be $\theta_D = 235 \text{ K}$ from $\beta = 0.75 \text{ mJ/mol K}^4$. The upper critical field H_{c2} was determined from the midpoint of the specific-heat transition, indicated by the line in the inset of Fig. 5.

The gradient $-dH_{c2}/dT$ was estimated by analyzing the M - T curve with magnetic fields, perpendicular ($H \parallel ab$) and parallel ($H \parallel c$) to the c axis, as well as the M - H and C_p - T curves. The values were found to be quite similar: 2653 Oe/K for H_{c2} from M - T ($H \parallel ab$), 2640 Oe/K for H_{c2} from M - T ($H \parallel c$), 2602 Oe/K for H_{c2} from M - H ($H \parallel c$), and 2702 Oe/K for H_{c2} from C_p - T ($H \parallel c$). In addition, the values are much larger than those previously obtained from polycrystalline samples,⁸ which are 840 and 830 Oe/K for H_{c2} from the M - H (T) and M - T (T) curves, respectively. The ThCr_2Si_2 -type BaNi_2As_2 compound was found to have a comparable $-dH_{c2}/dT$ value of $\sim 2260 \text{ Oe/K}$.¹⁵

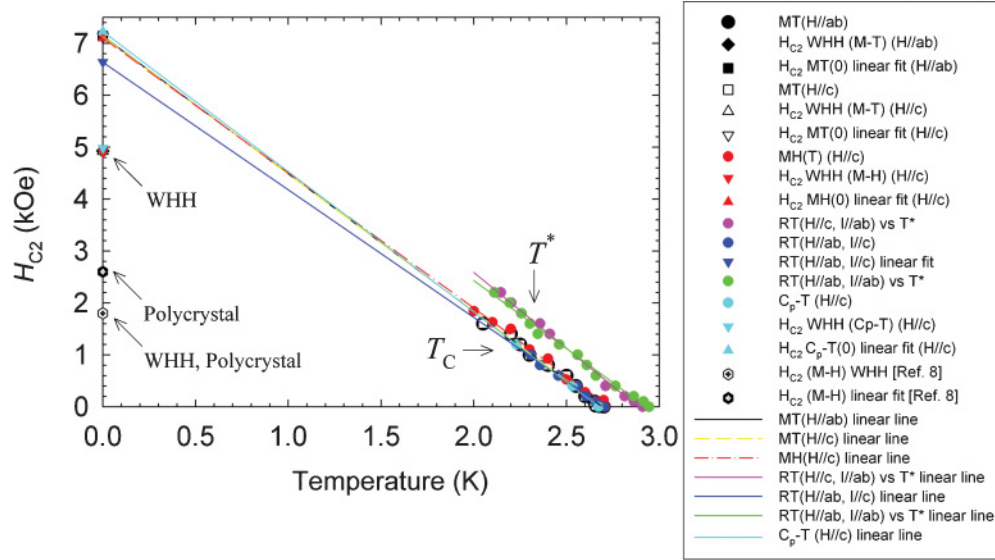


FIG. 6. (Color online) H - T diagram for the upper critical fields of a SrPd_2Ge_2 single crystal, determined from the various measurements in this paper (see text). Data from polycrystalline sample are from Ref. 8.

The upper critical fields, $H_{c2}(0)$, were estimated by a linear fit to be $H_{c2}^{\parallel c}(0)_{MT} = 7131$ Oe and $H_{c2}^{\parallel ab}(0)_{MT} = 7141$ Oe from the M - T curve. The coherence length values, $\xi_c = 21.45$ nm and $\xi_{ab} = 21.48$ nm, were calculated using Ginzburg-Landau (GL) relations, $H_{c2}^{\parallel c} = \Phi_0/2\pi\xi_{ab}^2$ and $H_{c2}^{\parallel ab} = \Phi_0/2\pi\xi_c\xi_{ab}$, where $\Phi_0 = 2.07 \times 10^{-7}$ Oe cm² is the flux quantum. The upper critical field at $T = 0$ K, which was determined by the Werthamer-Helfand-Hohenberg (WHH) theory,¹⁶ $H_{c2}(0)_{WHH} = -0.69T_c \left| \frac{dH_{c2}(T)}{dT} \right|_{T_c}$, was also calculated to be $H_{c2}^{\parallel c}(0)_{WHH} = 4921$ Oe and $H_{c2}^{\parallel ab}(0)_{WHH} = 4927$ Oe. Note that the upper critical field from the M - H curve was found to be similar to the values from the M - T curve: $H_{c2}^{\parallel c}(0)_{MH} = 7104$ Oe and $H_{c2}^{\parallel ab}(0)_{MH} = 4901$ Oe, respectively. From the C_p - T curve, the value of $H_{c2}(0)_{C_p-T} = 7230$ Oe was obtained, and $H_{c2}(0)_{C_p-T}^{WHH} = 4983$ Oe was determined based on the slope $-\frac{dH_{c2}}{dT} = 2702$ Oe/K and the WHH equation. In addition, the coherence length of $\xi_{GL}(0) = 21.34$ nm was obtained using the GL coherence length formula $\xi_{GL} = [\frac{\Phi_0}{2\pi H_{c2}(0)}]^{1/2}$. A similar upper critical field, $H_{c2}^{\parallel ab}(0)_{RT(I\parallel c)} = 6637$ Oe, was calculated from a linear fit of the R - T curve. The H_{c2} values from the data in this manuscript were collected and plotted in Fig. 6. In the figure, there seems to be almost no anisotropy (or very weak anisotropy) in the superconductivity of SrPd_2Ge_2 . The temperature, T^* , was also plotted, and appears to correlate well with the upper critical field $H_{c2}(T)$ and, equivalently, the superconductivity in SrPd_2Ge_2 .

Because the upper critical fields reported here are much smaller than those expected from the weak-coupling Pauli limiting effect, $H_p(0) \equiv 1.86T_c \cong 5$ T, the results suggest that the orbital effect, associated with diamagnetic supercurrents, is important in SrPd_2Ge_2 . This behavior resembles the case for the phosphorus-based Fe pnictide superconductors,^{6,17,18} but not the case for their As analog.^{12,19,20}

The weak anisotropic behavior in superconductivity has been previously reported in ThCr_2Si_2 -type pnictide superconductors, such as BaNi_2P_2 ,¹⁸ $(\text{Ba}_{1-x}\text{K}_x)\text{Fe}_2\text{As}_2$,¹⁹ and $\text{SrFe}_{1.85}\text{Co}_{0.15}\text{As}_2$ (Ref. 20) single crystals. According to these results, weak anisotropy was suggested as being universal in ThCr_2Si_2 -type structure compounds. Interestingly, weak anisotropy even in 111-type pnictide superconductors, LiFeAs ,²¹ and 11-type iron chalcogenide superconductors, $\text{Fe}_{1.11}\text{Te}_{0.6}\text{Se}_{0.4}$,²² was also reported. Therefore, the weak anisotropy in ThCr_2Si_2 -type pnictide is likely to be owing to the common nature of compounds that have a layer of FeAs or FeSe as the conducting path. This lack of anisotropy in SrPd_2Ge_2 can be understood from this point of view, and is also consistent with the band-structure calculation.¹⁴ Moreover, the Fermi surface (FS) calculation suggests a multisheet three-dimensional topology rather than two-dimensional-like FS topology in pnictide compounds. A further detailed theoretical and experimental study, such as angle-resolved photoemission spectroscopy (ARPES) to investigate the FS in this compound, would be interesting. Furthermore, electron (or hole) doping and chemical pressure experiments would also be valuable in order to study the variation of superconductivity in SrPd_2Ge_2 .

IV. SUMMARY

Single crystals of the ternary germanide superconductor SrPd_2Ge_2 ($T_c = 2.70$ K) were successfully fabricated using a metal self-flux method. Magnetization, electrical resistivity, and heat capacity were measured with the field along specific crystallographic directions, and very weak anisotropy was found between the fields perpendicular and parallel to the c axis. The upper critical field (H_{c2}) was found to be much higher than the values of the polycrystalline sample in Ref. 8. Interestingly, the anomalous temperature

dependence of resistivity in a temperature range of T_c ($=2.70$ K) $\leq T \leq T^*$ ($=2.90$ K) was observed with a current parallel to the c axis, whereas the resistivity perpendicular to the c axis shows just a slope change at T^* prior to a sharp superconducting transition at T_c . The origin of the anomaly is surmised to be related to the correlation of quasiparticles and Cooper-pair tunneling, and is currently under further investigation.

ACKNOWLEDGMENTS

The authors would like to acknowledge useful discussions with A. Kreyssig and P. Szabó, and thank B. Y. Kang for experimental assistance. This work was supported by the Ministry of Education, Science and Technology of Korea (Project No. R31-2008-000-10026-0) and by the Korea Science and Engineering Foundation (Grant No. R15-2008-006-01002-0).

-
- ¹N. D. Mathur, F. M. Grosche, S. R. Julian, I. R. Walker, D. M. Freye, R. K. W. Haselwimmer, and G. G. Lonzarich, *Nature (London)* **394**, 39 (1998).
 - ²O. Trovarelli, C. Geibel, S. Mederle, C. Langhammer, F. M. Grosche, P. Gegenwart, M. Lang, G. Sparn, and F. Steglich, *Phys. Rev. Lett.* **85**, 626 (2000).
 - ³P. Gegenwart, T. Westerkamp, C. Krellner, Y. Tokiwa, S. Paschen, C. Geibel, F. Steglich, E. Abrahams, and Q. Si, *Science* **315**, 969 (2007).
 - ⁴Marianne Rotter, Marcus Tegel, and Dirk Johrendt, *Phys. Rev. Lett.* **101**, 107006 (2008).
 - ⁵Kalyan Sasmal, Bing Lv, Bernd Lorenz, Arnold M. Guloy, Feng Chen, Yu-Yi Xue, and Ching-Wu Chu, *Phys. Rev. Lett.* **101**, 107007 (2008).
 - ⁶N. Berry, C. Capan, G. Seyfarth, A. D. Bianchi, J. Ziller, and Z. Fisk, *Phys. Rev. B* **79**, 180502(R) (2009).
 - ⁷Jian-Tao Han, Jian-Shi Zhou, Jin-Guang Cheng, and John B. Goodenough, *J. Am. Chem. Soc.* **132**, 908 (2010).
 - ⁸H. Fujii and A. Sato, *Phys. Rev. B* **79**, 224522 (2009).
 - ⁹K. A. Müller, M. Takashige, and J. G. Bednorz, *Phys. Rev. Lett.* **58**, 1143 (1987).
 - ¹⁰T. Ito, H. Takagi, S. Ishibashi, T. Ido, and S. Uchida, *Nature (London)* **350**, 596 (1991).
 - ¹¹P. Szabó, P. Samuely, J. Kačmarčík, A. G. M. Jansen, A. Briggs, A. Lafond, and A. Meerschaut, *Phys. Rev. Lett.* **86**, 5990 (2001).
 - ¹²S. R. Saha, N. P. Butch, K. Kirshenbaum, Johnpierre Paglione, and P. Y. Zavalij, *Phys. Rev. Lett.* **103**, 037005 (2009).
 - ¹³G. F. Chen, Z. Li, J. Dong, G. Li, W. Z. Hu, X. D. Zhang, X. H. Song, P. Zheng, N. L. Wang, and J. L. Luo, *Phys. Rev. B* **78**, 224512 (2008).
 - ¹⁴I. R. Shein, and A. L. Ivanovskii, *Physica B* **405**, 3213 (2010).
 - ¹⁵N. Kurita, F. Ronning, Y. Tokiwa, E. D. Bauer, A. Subedi, D. J. Singh, J. D. Thompson, and R. Movshovich *Phys. Rev. Lett.* **102**, 147004 (2009).
 - ¹⁶N. R. Werthamer, E. Helfand, and P. C. Hohenberg, *Phys. Rev.* **147**, 295 (1966).
 - ¹⁷F. Ronning, E. D. Bauer, T. Park, S.-H. Baek, H. Sakai, and J. D. Thompson, *Phys. Rev. B* **79**, 134507 (2009).
 - ¹⁸Y. Tomioka, S. Ishida, M. Nakajima, T. Ito, H. Kito, A. Iyo, H. Eisaki, and S. Uchida, *Phys. Rev. B* **79**, 132506 (2009).
 - ¹⁹H. Q. Yuan, J. Singleton, F. F. Balakirev, S. A. Baily, G. F. Chen, J. L. Luo, and N. L. Wang, *Nature (London)* **457**, 565 (2009).
 - ²⁰Seunghyun Khim, Jun Sung Kim, Jae Wook Kim, Suk Ho Lee, F. F. Balakirev, Yunkyu Bang, and Kee Hoon Kim, *Physica C* **470**, S317 (2010).
 - ²¹Yoo Jang Song, Jin Soo Ghim, Byeong Hun Min, Yong Seung Kwon, Myung Hwa Jung, and Jong-Soo Rhyee, *Appl. Phys. Lett.* **96**, 212508 (2010).
 - ²²Minghu Fang, Jinhua Yang, F. F. Balakirev, Y. Kohama, J. Singleton, B. Qian, Z. Q. Mao, Hangdong Wang, and H. Q. Yuan, *Phys. Rev. B* **81**, 020509(R) (2010).